JVI Journals.ASM.org

Aluminum Hydroxide Influences Not Only the Extent but Also the Fine Specificity and Functional Activity of Antibody Responses to Tick-Borne Encephalitis Virus in Mice

Juergen Zlatkovic, Georgios Tsouchnikas, Johanna Jarmer, Christian Koessl,* Karin Stiasny, Franz X. Heinz

Department of Virology, Medical University of Vienna, Vienna, Austria

Aluminum hydroxide is the most widely used adjuvant in human vaccines and serves as a potent enhancer of antibody production. Its stimulatory effect strongly depends on the adsorption of the antigen to the adjuvant, which may influence antigen presentation and, as a consequence, the fine specificity of antibody responses. Such variations can have functional consequences and can modulate the effectiveness of humoral immunity. Therefore, we investigated the influence of aluminum hydroxide on the fine specificity of antibody responses in a model study in mice using an inactivated purified virus particle, the flavivirus tick-borne encephalitis (TBE) virus, as an immunogen. To dissect and quantify the specificities of polyclonal antibodies in postimmunization sera, we established a platform of immunoassays using recombinant forms of the major target of neutralizing antibodies (protein E) as well as individual domains of E (DIII and the combination of DI and DII [DI+DII]). Our analyses revealed a higher proportion of neutralizing than virion binding (as detected by enzyme-linked immunosorbent assay) antibodies after immunization with aluminum hydroxide. Furthermore, the induction of antibodies to DIII, a known target of potently neutralizing antibodies, as well as their contributions to virus neutralization were significantly greater in mice immunized with adjuvant and correlated with a higher avidity of these antibodies. Thus, our data provide evidence that aluminum hydroxide can lead to functionally relevant modulations of antibody fine specificities in addition to its known overall immune enhancement effect.

Vaccines containing recombinant subunit antigens, protein toxins, or inactivated viruses are frequently supplied with adjuvants to increase their immunogenicity (1). Aluminum hydroxide, which is a potent enhancer of the serum antibody response via the stimulation of a strong $CD4^+$ T helper cell response (2, 3), is the most widely used adjuvant in human vaccines and is included, for example, in hepatitis A/B, Japanese encephalitis, tick-borne encephalitis, *Haemophilus influenzae* B, and tetanus toxoid vaccines (1). In general, aluminum salts are known to create a local inflammatory environment at the injection site, activating and attracting innate immune cells such as monocytes or dendritic cells, which enhance the activation of antigen-specific naive $CD4^+$ T helper cells in the lymph node (3, 4). Although the activation of the NLRP3 inflammasome has been proposed to play a key role in the initiation of the inflammatory response upon aluminum hydroxide administration (5–7), some controversy exists regarding whether the inflammasome is indeed required for the adjuvant effect *in vivo* (8–11). Recently, the aluminum hydroxide-induced release of host DNA has been shown to provide an immunostimulatory signal (12) and to increase the interaction between $CD4^+$ T cells and antigen-presenting cells (13).

In addition to these inflammatory stimuli, adsorption of the antigen to aluminum hydroxide is generally accepted as being crucial for its adjuvant effect (3, 4, 14). In the case of protein antigens, this interaction can lead to changes in the secondary or tertiary structure and can affect protein stability (15–18). Since adsorption-induced effects on protein structure can potentially modulate the fine specificities and, consequently, the functional activities of antibodies elicited by immunization, such changes can affect the effectiveness of vaccination. Therefore, the main objective of our model study was to investigate to what extent aluminum hydroxide can influence antibody fine specificity and functional activity. For this purpose, we conducted a mouse immunization study using formalin-inactivated tick-borne encephalitis (TBE) virus as an immunogen, either alone or after adsorption to aluminum hydroxide (−Alu and +Alu groups). This adjuvant is also used in the commercially available TBE vaccines in Europe and Russia (1).

TBE virus is a member of the genus *Flavivirus* (family *Flaviviridae*), which comprises other important human-pathogenic viruses, such as dengue, West Nile (WN), yellow fever, and Japanese encephalitis viruses (19). These small isometric viruses are composed of a structurally ill-defined nucleocapsid containing the positive-stranded RNA genome and a lipid envelope carrying 180 copies of glycoprotein E and the small membrane-associated protein M (20) (Fig. 1A). For several flaviviruses, the structure of E has been determined using X-ray crystallography (Fig. 1B) (21–25), and cryo-electron microscopy of viral particles revealed a specific icosahedral arrangement of E at the viral surface (26–30). The M protein is located beneath the E protein dimer (28). The external part of E (sE), lacking the hydrophobic C-terminal double membrane-spanning anchor and the membrane-proximal region (called the stem), is composed of three distinct structural domains (DI, DII, and DIII) (Fig. 1B) (21–25). Because of its essential func-

Received 20 June 2013 Accepted 27 August 2013

Published ahead of print 4 September 2013

Address correspondence to Franz X. Heinz, Franz.X.Heinz@meduniwien.ac.at.

* Present address: Christian Koessl, Boehringer Ingelheim RCV GmbH & Co KG, Vienna, Austria.

Supplemental material for this article may be found at http://dx.doi.org/10.1128/JVI.01690-13.

doi:10.1128/JVI.01690-13

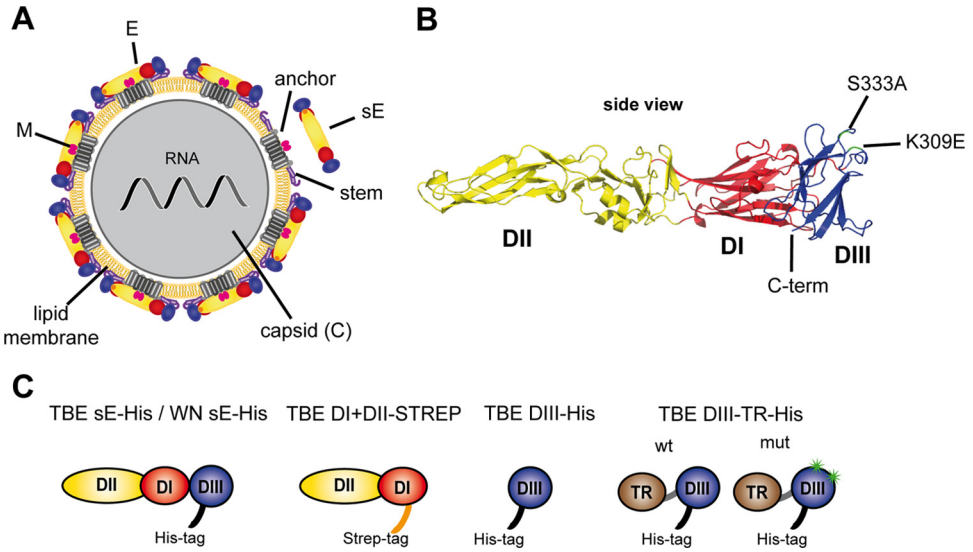

FIG 1 Structure of flaviviruses and recombinant antigens used for serological analyses. (A) Schematic model of the flavivirus virion. The capsid, which is surrounded by a lipid membrane, contains the viral RNA genome and multiple copies of the capsid protein C. Proteins E and M are anchored in the viral membrane and form an icosahedral lattice. A soluble form of an E protein (sE) dimer lacking the stem and anchor regions is indicated. (B) Ribbon diagram of the soluble E protein monomer of TBE virus (Protein Data Bank [PDB] code 1SVB; side view) (22). In DIII, the positions of amino acid replacements used to generate the so-called DIII lateral ridge mutant are indicated and highlighted in green. (C) Schematic representations of recombinant proteins used for serological analyses. Color code (A to C): protein M, pink; protein E, DI, red; DII; yellow; DIII, blue; anchor, gray; stem, purple; capsid protein, gray; RNA, dark gray; lipid membrane, yellow; His tag, black; Strep tag, orange; TR (thioredoxin), brown; and DIII-lr mutations, green.

tions in receptor binding and entry (20), E is the major target of virus neutralizing antibodies, and their induction correlates with protection against flavivirus-induced disease, including TBE (31–33). Studies using monoclonal antibodies (MAbs) demonstrated that binding to each of the three domains of E can lead to virus neutralization, and highly potent antibodies were shown to be directed at a surface-exposed epitope within DIII, the so-called DIII lateral ridge (DIII-lr) epitope (34). In mice (35, 36), in contrast to humans (36–40) or horses (41), DIII-specific antibodies comprise a significant fraction of the polyclonal antibody response following flavivirus infection and vaccination.

In this study, we present a detailed analysis of the influence of aluminum hydroxide on the antibody response and its fine specificity in a mouse immunization study with inactivated TBE virus. Using a set of recombinant antigens, we were able to quantify the extent and functionality of antibody responses to individual domains (DIII and the combination of DI and DII [DI+DII]) of E. We demonstrate that the proportion of neutralizing antibodies relative to virion binding antibodies (as determined by enzyme-linked immunosorbent assay [ELISA]), as well as the contribution of DIII-reactive antibodies to virus neutralization, were significantly higher in the +Alu than the −Alu group. We also found that aluminum hydroxide affected the relative proportion of antibodies to a specific antigenic site in DIII, corresponding to the DIII-lr epitope in West Nile virus (42). Taken together, our results strongly indicate that aluminum hydroxide not only leads to an overall enhancement of antibody responses but also can modulate its fine specificity, i.e., the extent of responses to distinct sites within a protein antigen. Such variations can have implications for the quality of vaccine-induced immunity.

MATERIALS AND METHODS

Production of purified formalin-inactivated TBE virus. Virus production and purification was performed as described previously (43). In brief, primary chicken embryo cells were infected with the TBE virus strain Neudoerfl (GenBank accession no. U27495). The supernatant was harvested 24 h postinfection, clarified by low-speed centrifugation, and treated with 37% formalin, at a final dilution of 1:2,000, for 24 h at 37°C. The inactivated virus was pelleted by ultracentrifugation and purified by rate zonal centrifugation, followed by equilibrium sucrose density gradient centrifugation. The absence of infectious virus in this preparation was confirmed by the most sensitive indicator of TBE virus infectivity, i.e., intracerebral inoculation of Swiss albino suckling mice (strain OF-1), which were monitored for 14 days postinoculation. Mouse experiments were approved by the ethics committee of the Medical University of Vienna and the Austrian Federal Ministry of Science (permit number BMBWK-66.009/0249-BrGT/2005). Sample analysis by SDS-PAGE (5% phosphate gels according to Maizel [44]) and Coomassie staining (Fig. 2A), as well as Western blotting (Fig. 2B), revealed the structural proteins E, C, and M together with oligomeric bands of E and C as a result of protein cross-linking by formalin.

Preparation of immunogens and mouse immunization experiments. Mouse experiments were performed in strict accordance with the guidelines of the Federation of European Laboratory Animal Science Associations (FELASA) and Austrian federal law. The protocol was approved by the ethics committee of the Medical University of Vienna and the Austrian Federal Ministry of Science and Research (permit number BMBWK-66.009/0057-BrGT/2006).

For the immunization of mice, formalin-inactivated and purified TBE virus was used at a protein concentration of 10 μg/ml in a buffer containing 0.05 M triethanolamine and 0.1 M NaCl, pH 8.0 (TAN buffer), either without or with 0.2% aluminum hydroxide adjuvant (aluminum hydroxide gel; Sigma-Aldrich, St. Louis, MO). The adjuvanted immunogen was prepared by dropwise addition of inactivated TBE virus to aluminum hydroxide under constant mixing on an orbital shaker (500 rpm; 25°C) and further incubation for 30 min. Adsorption of the inactivated virion to aluminum hydroxide was controlled by pelleting the adjuvant from the slurry (20,000 × *g* for 10 min) and analyzing the clear supernatant for the presence of residual viral antigen by ELISA (45). This analysis revealed quantitative virus adsorption under the conditions used.

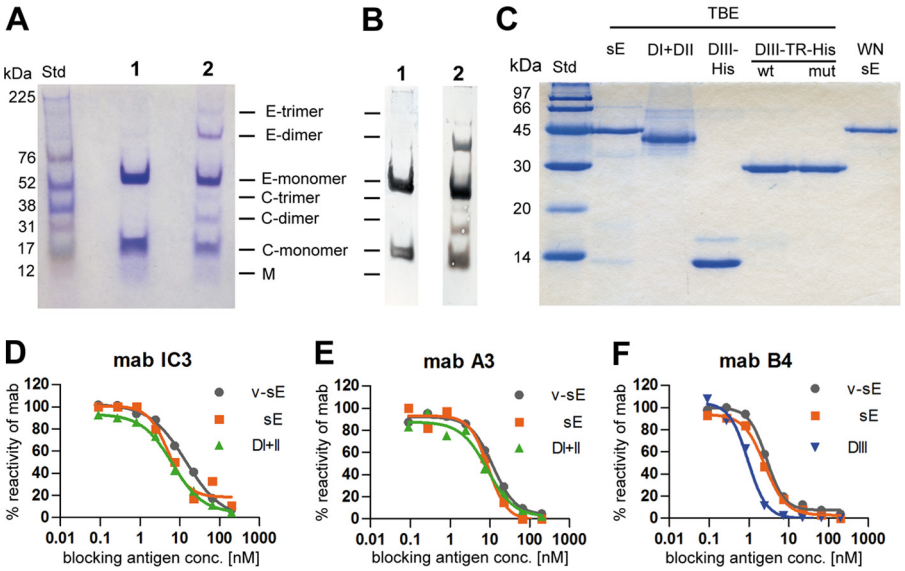

FIG 2 Quality controls of antigens used in the study. (A) Coomassie-stained SDS-PAGE (5% phosphate gel) (44) and Western blotting (B) with a polyclonal mouse serum specific for C and E proteins (lanes 1, purified live virus; lanes 2, formalin-inactivated virus used for immunization). Monomeric and formalin cross-linked oligomeric bands of C and E proteins are labeled. (C) Coomassie-stained SDS-PAGE (15% Laemmli gel) of recombinant proteins used in ELISA and depletion assays. Molecular mass standards (Std) are indicated on the left. (D to F) Blocking ELISAs with MAbs specific for DI (IC3), DII (A3), and DIII (B4) and recombinant antigens (sE, orange; DI+II, green; DIII, blue) compared to sE isolated from purified live virions (v-sE, gray) (22).

Groups of 10 C57BL/6N mice (Charles River Laboratories, Sulzfeld, Germany) were immunized subcutaneously three times with 100 μl/mouse of either the nonadjuvanted or the adjuvanted immunogen (corresponding to 1 μg inactivated TBE virus per dose), with intervals of 14 days between the vaccinations. Two weeks after the third immunization, blood samples were taken from the tail vein using microvette 200 capillaries (Sarstedt), and equal aliquots of sera from individual mice were pooled for further analyses.

Expression and purification of recombinant proteins. (i) Recombinant TBE, WN sE, and TBE DI+DII proteins. DNA cassettes encoding the soluble forms of recombinant TBE sE and WN sE, both C-terminally truncated after amino acid 400, were cloned into the pMT/Bip/V5-His expression vector (Life Technologies), which contains the *Drosophila* export signal sequence (BiP) and a C-terminal His tag as described in reference 35. Recombinant TBE DI+DII (C-terminally truncated after amino acid 302) was cloned using the pT389 expression vector (kindly provided by Thomas Krey and Felix Rey, Institut Pasteur, France) containing the *Drosophila* BiP signal sequence, an enterokinase cleavage site, and a double Strep tag. The sE or DI+DII expression vector was cotransfected into *Drosophila* Schneider 2 (S2) cells together with a plasmid carrying a blasticidin resistance gene according to the manufacturer's protocol (Invitrogen), allowing for the selection of stably transfected cells. Protein expression was induced by the addition of 500 μM $CuSO_4$ to the cell culture medium, and the supernatants were harvested 7 to 11 days postinduction. His-tagged TBE and WN virus sE proteins were purified by immunoaffinity chromatography using the monoclonal antibody (MAb) 4G2 as described previously (35). The bound sE proteins were eluted from the column by 20 mM glycine, pH 2.7, and immediately back neutralized to pH 8.0. The Strep-tagged TBE DI+DII protein was purified using Strep-Tactin columns (IBA) according to the manufacturer's protocol.

(ii) Recombinant DIII proteins. ***(a)*** **Wild-type (wt) DIII-TR-His.** DIII proteins of TBE virus strain Neudörfl (amino acids 302 to 398 of E protein) were expressed in *Escherichia coli* strain BL21 as a fusion protein with thioredoxin (TR) carrying a C-terminal His tag using the pET 32a Xa/LIC vector (Novagen) as described previously (35). After clarification of *E. coli* cell lysates, the DIII-TR-His protein was purified by Ni^{2+} affinity chromatography (GE-Healthcare Life Sciences).

(b) **lr mut DIII-TR-His.** The TBE DIII-TR-His-lr loss-of-function mutant (mut) was constructed in analogy to the WN DIII-lr mutant described previously (36). The corresponding residues in TBE DIII were identified by sequence and structural alignments based on the previously published crystal structures of the TBE and WN sE proteins (21, 22). Mutations at amino acid residues 309 (S replaced by A) and 333 (K replaced by E) were introduced into the TBE DIII-TR-His wt DNA clone by site-directed mutagenesis according to the manufacturer's protocol (Invitrogen). The protein was expressed and purified as described above for the wt protein.

(c) **DIII-His.** The isolated recombinant DIII-His was obtained by proteolytic cleavage of the TBE DIII-TR-His fusion protein with factor Xa essentially as described previously for WN DIII-His (35).

(iii) Quality control of recombinant proteins. The recombinant proteins (schematically depicted in Fig. 1C) were checked for purity by 15% SDS-PAGE (Fig. 2C). The oligomeric structure of the sE proteins was confirmed to be a dimer in the case of TBE virus sE and a monomer in the case of WN virus sE by cross-linking and sedimentation analyses as described previously (35) (data not shown).

Proper folding of the recombinant proteins was verified with conformation-dependent neutralizing MAbs specific for DI (IC3), DII (A3), and DIII (B4) in a blocking ELISA (46) by comparison to sE isolated from purified live TBE virus (22). In brief, serial dilutions of the recombinant antigens and virion-derived sE were preincubated with a fixed dilution of the respective MAbs before transfer to the wells of microtiter plates coated with purified inactivated TBE virus. Antibodies bound to the viral antigen on the solid phase (i.e., not blocked by the antigens in solution) were detected by peroxidase-labeled rabbit anti-mouse IgG as described below for the 3-layer ELISAs. The results were expressed as percent absorbance in the absence of the blocking antigen (percent reactivity of MAb) (Fig. 2D to F).

Three-layer ELISAs. Untreated 96-well microtiter plates (Nunc) were coated overnight with 25 ng/well of formalin-inactivated TBE virus, and Nunc Maxisorp 96-well plates were coated with 50 ng/well of recombinant TBE DI+DII and DIII-TR-His wt and mut in carbonate buffer, pH 9.6, at 4°C. Three-fold serial dilutions of the mouse serum pools, starting at a dilution of 1:100, were added to the coated plates and incubated for 1

h at 37°C. As negative controls, sera from naive mice were included. The bound antibodies were detected using peroxidase-labeled rabbit anti-mouse IgG as previously described (47). Absorbance values were determined at 490 nm. For quantifying the results, a panel of eight negative sera was included in all assays and used for determining cutoff values. These were set at the mean absorbance of the negative controls plus three standard deviations, as previously described (48). Reactivities above the cutoff were considered positive and were used for titer calculation by curve fitting using a four-parameter logistic regression with GraphPad Prism 5 software (GraphPad Software Inc., San Diego, CA). Each serum pool was tested in at least three independent experiments.

Comparison of relative avidities in 3-layer ELISAs. To measure relative avidities of specific antibodies in the postimmunization sera, we have established urea-ELISAs which are used for the differentiation of low- and high-avidity polyclonal sera (49–51). For this purpose, sera were analyzed in 3-layer ELISAs as described above, except that an additional washing step with 4 M urea was included after incubation of the serum dilutions with antigens, essentially as previously described (52). Serum antibody titers were determined at an absorbance cutoff of 1.0 after curve fitting with a four-parameter logistic regression using GraphPad Prism 5 (GraphPad Software Inc., San Diego, CA). Relative avidities were expressed as the percentage of titers obtained with and without urea.

Four-layer ELISAs. ELISA analyses using His-tagged recombinant proteins (TBE and WN virus sE- and DIII-His) were performed as previously described (35). In brief, Nunc 96-well Maxisorp microtiter plates were coated with 50 ng/well of a rabbit anti-His tag antibody (QED Biosciences) overnight at 4°C in carbonate buffer, pH 9.6. Twenty-five ng/well of recombinant His-tagged sE and 50 ng/well of DIII proteins were added to the plates and incubated for 1 h at 37°C. Three-fold serial dilutions of mouse sera, starting at a dilution of 1:100, were added and incubated for 1 h at 37°C. The bound antibodies were detected using a peroxidase-labeled goat anti-mouse IgG conjugate (Pierce). The establishment of titration curves and calculations of ELISA titers were performed as described previously for the 3-layer ELISAs.

Antibody depletion assays using recombinant TBE virus DIII-His. Depletion of DIII-specific antibodies was performed as previously described (35). In brief, 1 μg of recombinant isolated DIII-His was bound to 1 mg of paramagnetic Co^{2+}-coated Dynabeads (His tag isolation and pulldown; Life Technologies) for 30 min on an orbital shaker (1,000 rpm) at room temperature. After pelleting by magnetic force and washing with pull-down buffer, the beads were incubated with postimmunization serum pools (prediluted 1:5 in phosphate-buffered saline [PBS]) for 1 h at 37°C. The beads were subsequently pelleted again by magnetic force and the depleted serum was collected. To achieve quantitative removal of DIII-reactive antibodies, the depletion procedure was performed three times. Unloaded beads were used as a control to confirm the absence of nonspecific binding of serum antibodies to the beads.

TBE virus neutralization assay. TBE virus neutralizing activity of pooled mouse sera was determined in a 96-well plate format with baby hamster kidney cells (ATCC BHK-21) using an assay that uses a constant dilution of serum (1:100) and varying amounts of virus. This assay format was chosen because it required less than half of the serum volume required for other formats; therefore, it allowed the conducting of necessary repetitions of pre- and postdepletion NTs with the small amounts of mouse sera available. For these analyses, we used TBE virus strain HYPR (GenBank accession no. U39292), which yielded highly reproducible growth curves optimal for curve fitting by nonlinear regression.

Heat-inactivated (56°C for 30 min) mouse sera at a fixed dilution of 1:100 were mixed with 10-fold serial virus dilutions (starting with $10^{6.2}$ 50% tissue culture infectious doses) and incubated for 1 h at 37°C. Virus mixed with medium only served as the virus control, and negative mouse sera and TBE virus-specific monoclonal antibodies were used as negative and positive controls, respectively. BHK-21 cells were then added to the virus-antibody mixture and incubated overnight at 37°C. The culture supernatants were replaced by fresh medium 16 to 20 h postinfection, and incubation was continued for 24 h at 37°C. The culture supernatant was then harvested and the virus was detected using 4-layer ELISA as described previously (53).

Virus titration curves were established by curve fitting using a four-parameter logistic regression with GraphPad Prism 5 software (GraphPad Software Inc., San Diego, CA). The virus titer of each curve was read at the half absorbance saturation point of the titration curves, and neutralizing activity was defined as the fold reduction of virus titers obtained after addition of test sera compared to titers after addition of negative sera. The assays were performed three times with all samples tested in duplicate, and the results are expressed as the means of these three repetitions.

Statistical analyses. Data were analyzed using GraphPad Prism software, version 5 (Graph Pad Software Inc., San Diego, CA). Two-tailed *t* tests were used to compare antibody titers, ratios of antibody titers, ELISA avidities, and neutralizing activities. Differences were considered significant when the *P* value was less than 0.05.

RESULTS

Mouse immunization and overall antibody response. To investigate the influence of aluminum hydroxide on the antibody response to TBE virus, two groups of 10 mice were immunized with inactivated TBE virus either without (−Alu) or with (+Alu) aluminum hydroxide as described in Materials and Methods. Pools of postimmunization sera were used for all further analyses. First, the overall virion-specific antibody response was determined by virion ELISA and virus neutralization (NT) assays. The original ELISA data (mean absorbance values of all dilutions of postimmunization sera and the 1:100 dilutions of negative sera used for cutoff calculation; see Materials and Methods) are provided as Data Set S1 in the supplemental material. As shown in Fig. 3, the specific antibodies in the +Alu pool were substantially higher in both the virion ELISA (Fig. 3A) and the neutralization assay (Fig. 3B), consistent with the well-known adjuvant effect of aluminum hydroxide. However, the difference in titers was significantly more prominent in NT than in the virion ELISA, indicating a disproportionally higher neutralizing potency of the antibodies induced in the presence of the adjuvant (Fig. 3C). Because aluminum hydroxide has been previously shown to increase the avidity of antibody responses (54–56), we analyzed the relative avidities of the postimmunization sera in virion ELISA employing a urea wash step as described in Materials and Methods. Although there was a tendency to higher avidity in the +Alu group, this difference was not significant (Fig. 3D).

Fine specificity of the antibody response to E. To dissect the antibody response and to quantify the contribution of antibody subsets to virus neutralization, we established immunoassays with a set of recombinant antigens, which are schematically displayed in Fig. 1C. These included the following TBE virus proteins: sE, DI+DII, and DIII. Additionally, we included sE of the related WN virus for determining broadly flavivirus cross-reactive antibodies. The results obtained in ELISAs with these antigens are shown in Fig. 4. It has to be emphasized that these ELISAs have different formats and sensitivities and do not allow direct quantitative comparisons between the assays. However, they do allow comparisons between the −Alu and +Alu group with respect to the relative amounts of antibodies reacting in the different ELISAs. The original ELISA data (mean absorbance values of all dilutions of postimmunization sera and the 1:100 dilutions of negative sera used for cutoff calculation; see Materials and Methods) are provided as a supplemental data set. As expected, the antibody response against all antigens was higher in the +Alu group (Fig. 4A).

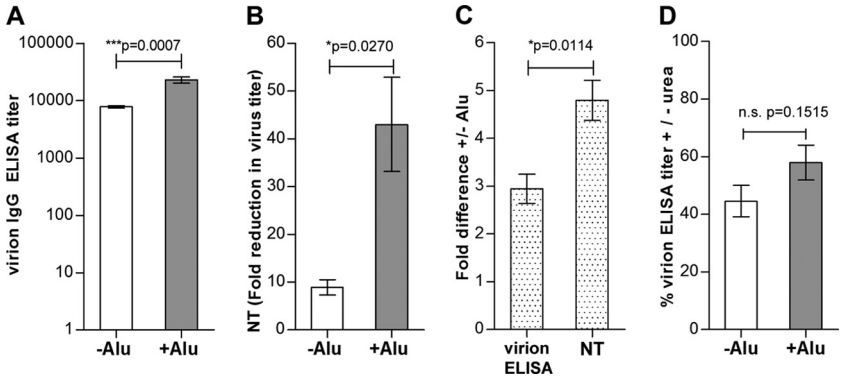

FIG 3 TBE virion-specific antibody response after immunization without and with aluminum hydroxide (−Alu and +Alu, respectively). Virion ELISA (A), NT (B), and fold difference of titers (C) obtained with the +Alu serum pool compared to the −Alu serum pool in virion ELISA and NT. (D) Virion ELISA avidities. The data represent the means from at least three independent experiments, and error bars indicate the standard errors of the means. n.s., not significant.

However, the DIII antibody titers were disproportionally increased compared to the virion titers in the +Alu serum pool, and this difference was significant (Fig. 4B). No comparable effect was found with the other antigens (Fig. 4B). These results indicate the induction of a higher proportion of DIII-specific antibodies after immunization with aluminum hydroxide.

Previous studies with MAbs or mouse postinfection sera of dengue (57) and WN (36, 42, 58) viruses highlighted the significance of a surface-exposed antigenic region, the so-called DIII lateral ridge (DIII-lr), as an important target of potently neutralizing antibodies. As a further measure of possible modulations of antibody fine specificities, we assessed the antibody response to the corresponding region on the lr of the TBE virus DIII with an lr mutant DIII (Fig. 1B and C) using 3-layer ELISA (see Materials and Methods).

In control experiments, we ensured that both wt and mut DIII-TR-His fusion proteins were coated equally well to microtiter plates by the use of an anti-His tag MAb (Fig. 5B), thereby allowing quantitative comparisons to be made. We also demonstrated that the mutations had selectively destroyed the epitopes of the DIII-specific MAbs B1 and B4 but not those of B2 and B3 (59, 60) (Fig. 5C to F). The results obtained with the serum pools from the −Alu and +Alu groups in ELISAs with wt and lr mutant DIII are shown in Fig. 6A and B. The reactivity with the mutant was reduced by 35% for the −Alu serum pool but only by 14% for the +Alu serum pool (Fig. 6A). Since there was no significant difference in avidity for the mutant DIII protein (Fig. 6B), this result suggests that the proportional amount of DIII-lr antibodies was approximately two times higher in the −Alu serum pool.

Contribution of DIII-specific antibodies to virus neutralization. Because of the differences in fine specificity observed between the −Alu and +Alu groups and the importance of DIII antibodies to virus neutralization (35, 36), we determined the contribution of DIII-specific antibodies to virus neutralization using antibody depletion with recombinant DIII (see Materials and Methods). The removal of DIII-specific antibodies was confirmed in the DIII ELISA, which showed quantitative depletion of DIII-specific antibodies in both serum pools (Fig. 7A). In the virion ELISA, this depletion resulted in the removal of similar amounts of virion-specific reactivity, 25 and 28% in the −Alu and +Alu serum pools, respectively (Fig. 7B). However, a significant difference was observed with respect to the effect of DIII antibody depletion on virus neutralization. Whereas 68% of NT activity was removed from the +Alu group, virtually no effect was observed in the −Alu group (Fig. 7C). The original neutralization curves used for these calculations are displayed in Fig. 7E and F. These results show that the DIII-specific antibodies, although contributing to the same extent to virion ELISA reactivity in both groups, differ strongly with respect to their contribution to neutralizing activity. DIII avidity ELISAs (Fig. 7D) revealed a significantly higher avidity in the +Alu group, which can, at least partially, explain the differences in the NT depletion analyses.

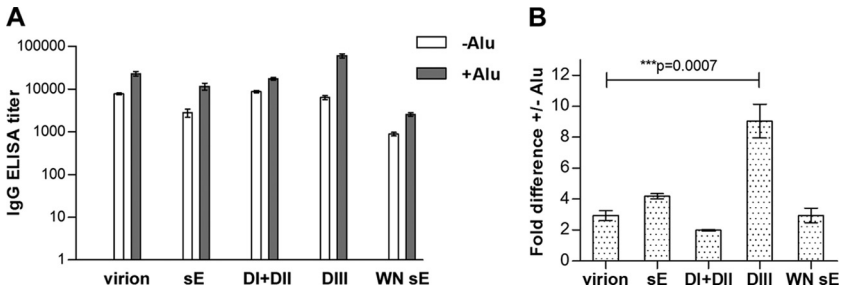

FIG 4 ELISA reactivities with virion and recombinant antigens of −Alu and +Alu serum pools. (A) ELISA titers against virion, soluble recombinant E (sE), DI+DII, and DIII of TBE virus and recombinant WN virus sE. (B) Fold difference of titers obtained with the +Alu serum pool compared to the −Alu serum pool in virion and recombinant protein ELISAs. The data represent the means from at least three independent experiments, and error bars indicate the standard errors of the means.

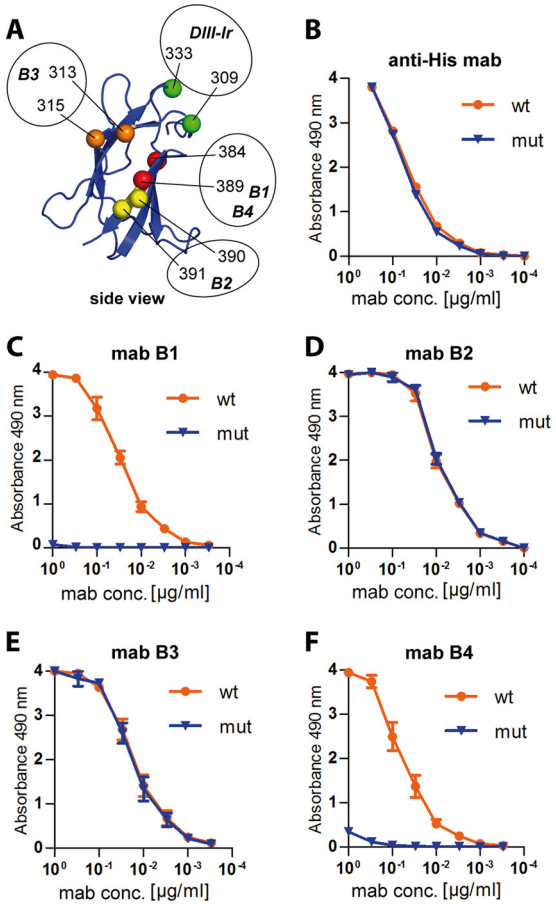

FIG 5 (A) Ribbon diagram of DIII (side view) with amino acid positions affecting the binding of DIII-specific MAbs (B1 to B4) highlighted by colored spheres: red, B1 and B4 (59, 72); yellow, B2 (46); orange, B3 (unpublished data). The newly generated DIII-lr mutant contains replacements at amino acid positions 309 and 333 (highlighted in green). (B to F) Titration curves of His tag-specific and TBE DIII-specific MAbs. MAb anti-His tag (B), MAb B1 (C), MAb B2 (D), MAb B3 (E), and MAb B4 (F) were used in ELISA using wild-type (wt; orange line) and DIII-lr mutant (mut; blue line) TBE-DIII-TR-His as antigens. The data represent the means from three independent experiments, and the error bars indicate the standard errors of the means.

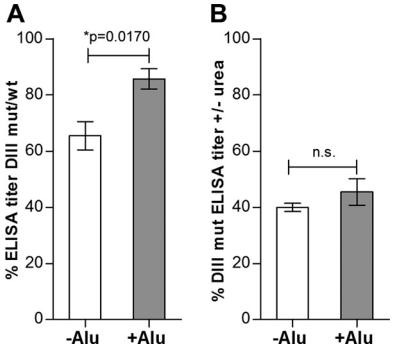

FIG 6 Antibody response to the TBE DIII-lr epitope. (A) Reduced reactivity of −Alu and +Alu serum pools with the DIII-lr mutant, expressed as a percentage of the DIII wt ELISA reactivity. (B) Relative avidities of −Alu and +Alu postimmunization sera for the DIII-lr mutant. The data represent the means from at least three independent experiments, and error bars indicate the standard errors of the means.

DISCUSSION

The capacity of aluminum salts to increase antibody responses is extensively documented and forms the basis for their widespread use as adjuvants in human and veterinary vaccines (61, 62). However, it is largely unknown whether the addition of such adjuvants to protein antigens can also modulate the fine specificity of antibody responses and affect the relative proportions of antibody populations, directed to different antigenic sites in the same protein, in postvaccination sera. Because such effects can also influence the functionality of immune responses, we have addressed this specific question in our study using a relatively simple virus particle, the flavivirus TBE virus (Fig. 1A), as an immunogen. The key finding of our work was that the use of aluminum hydroxide during immunization can exert a substantial influence on the composition and characteristics of antibodies induced, specifically on their reactivities with single protein domains, which also impact the functional activities of these antibodies. This principal conclusion is based on several lines of experimental evidence obtained through the comparative analysis of sera from mice immunized with inactivated TBE virus alone (−Alu group) or in the presence of aluminum hydroxide (+Alu group). This evidence included the following. (i) The increase of antibody titers by the addition of aluminum hydroxide was significantly higher in NT than in virion ELISA (Fig. 3C), suggesting a stronger focusing of the antibody response to epitopes most critical for virus neutralization. (ii) In studies with the related dengue and West Nile viruses, antibodies to domain III of E (57, 58, 63, 64) were shown to dominate in murine West Nile virus postinfection and postvaccination responses (35, 36). Consistent with the importance of such antibodies for virus neutralization and the higher specific neutralizing activity of sera from the +Alu group, we observed that these contained a significantly higher proportion of DIII-specific antibodies than the −Alu group (Fig. 4). (iii) In addition to this quantitative difference, we identified an important difference with respect to the functional activities of DIII-specific antibodies contained in the two serum pools. Approximately 68% of the total neutralizing antibody activity could be removed from the +Alu pool by recombinant DIII (Fig. 7C and F). This figure is in complete concordance with a recent mouse immunization study with the related West Nile virus (35) (which also used C57BL/6 mice and aluminum hydroxide as an adjuvant) and demonstrated that approximately 65% of the total neutralizing activity was due to DIII-specific antibodies. Thus, the data corroborated the functional dominance of these antibodies, at least after immunization of C57BL/6 mice, in the presence of aluminum hydroxide. However, a substantially different pattern was observed in the −Alu serum pool, in which the DIII-specific antibodies, although present, did not contribute to the neutralizing activity of the serum to any measureable extent (Fig. 7C and E).

Two additional sets of experimental data were suggestive of an adjuvant-induced modulation of antibody fine specificity. First, we demonstrated that the overall avidity of DIII antibodies was significantly higher in the +Alu than in the −Alu group (Fig. 7D), and although not statistically significant, there was also a tendency for a higher avidity against the whole virus (Fig. 3D). An increase of overall avidity through the use of aluminum salts as adjuvants has previously been described in immunization studies in mice and humans (54, 55, 65). Second, through the use of a mutant DIII with modifications at the so-called lateral ridge epitope originally

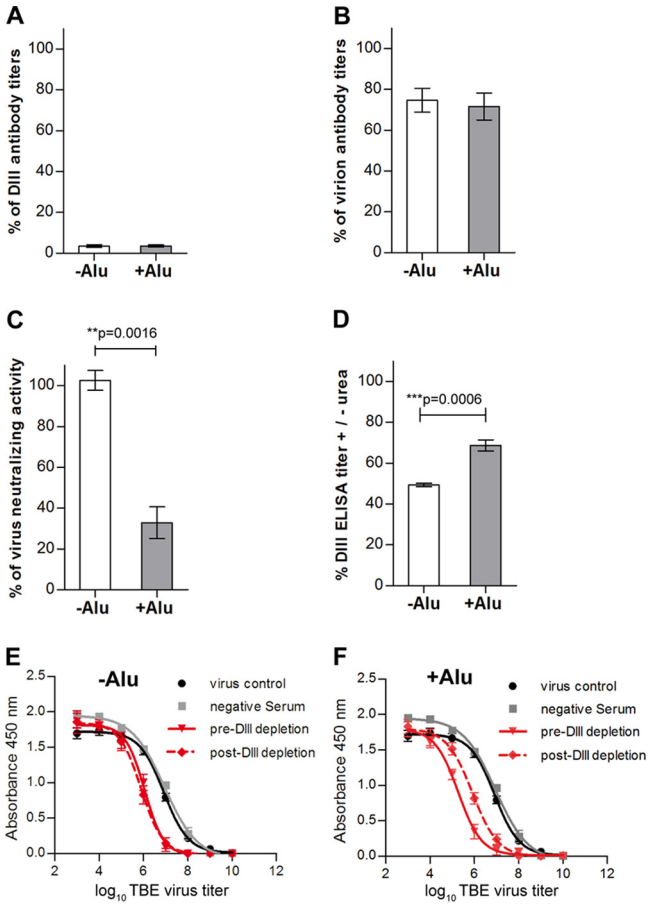

FIG 7 ELISA and NT analyses of −Alu and +Alu serum pools after depletion with recombinant DIII. (A) Percent remaining reactivity after antibody depletion with DIII, as determined by DIII ELISA. (B) Percent remaining reactivity after antibody depletion with DIII as determined by virion ELISA. (C) Percent remaining reactivity after antibody depletion with DIII as determined by TBE virus neutralization assay based on the data presented in panels E (−Alu) and F (+Alu). (D) Relative avidities of DIII antibodies in the postimmunization sera determined by avidity ELISA using DIII as an antigen. (E and F) NT virus titration curves of −Alu (E) and +Alu (F) serum pools before (red solid lines) and after (red dotted lines) antibody depletion with DIII. Black and gray curves represent the virus control incubated without antibody and with a negative-control serum pool of 10 naive mice, respectively. The data represent the means from at least three independent experiments, and error bars represent the standard errors of the means.

described in the West Nile virus system (36), we found that the −Alu group had a higher proportion of antibodies against this specific epitope than the +Alu group. Although the biological significance of such subtle differences presently is not clear, these data further corroborate the conclusion that aluminum hydroxide can modulate the fine specificities of antibody responses.

There is an obvious discrepancy between the proportion of DIII-specific antibodies determined directly by DIII ELISA (Fig. 4B) and DIII depletion (Fig. 7B). The data shown in Fig. 4B indicate that the +Alu serum pool contains a higher proportion of DIII antibodies than the −Alu pool, whereas no such difference was found in the depletion experiment, in which the apparent content of DIII antibodies was approximately 25% of the total virion-reactive antibodies in both instances. These seemingly discrepant results may be due to the weaker avidity of DIII-reactive antibodies induced in the absence of aluminum hydroxide, which have an increased likelihood to remain undetected by ELISA, because this assay favors high-avidity binders due to the many washing steps in the presence of detergent (66). Depletion analysis, on the other hand, involves the use of a large excess of antigen and three consecutive rounds of depletion (see Materials and Methods); thus, it is favorable for detecting low-avidity antibodies.

Mechanistically, the influences on antibody fine specificity observed in our study are likely a consequence of antigen adsorption to aluminum hydroxide, which has been shown to be crucial for its adjuvant effect (3, 4, 14). Indeed, in our experiments the antigen was completely adsorbed immediately after mixing with the adjuvant (data not shown). Previous studies have revealed that the interaction with aluminum hydroxide, which strongly depends on the properties of the antigen, buffer composition, pH, and physicochemical properties of the aluminum preparation used, can affect the structure of protein immunogens (15–18). Flavivirus particles are probably especially prone to adsorption-related structural effects, since the organization of their E proteins in the viral membrane is subject to dynamic changes (29, 30, 67), can be fixed in different configurations (e.g., by the interaction with specific antibodies [67]), and can undergo extensive temperature-dependent rearrangements (29, 30, 67). Interactions of aluminum hydroxide with the viral envelope and possible structural changes or the fixation of the flexible E protein subunits in a certain configuration may be one explanation for the higher proportion of DIII antibodies in ELISA (Fig. 4) and their increased contribution to virus neutralization (Fig. 7C). Some of the observations may also be due to effects of elution from the adjuvant in the interstitial fluid (68–70). Since aluminum hydroxide was found in secondary lymphoid organs up to 28 days after immunization (71), it is possible that antigen desorption is incomplete under physiological conditions, and certain epitopes may still be masked by the adjuvant to various extents when encountering B cells.

In conclusion, the data presented here reveal additional complexities of the immunological activity of aluminum hydroxide that can impact its efficacy as an adjuvant. Although we assume that the overall conclusions of our work can be generalized, the specific effects are likely to be dependent on the unique structural property of each immunogen and are largely unpredictable. Future studies should address questions of structure-specific factors (e.g., protein stability and small versus complex antigens), host-specific effects (e.g., mice versus humans), and the contribution of individual-specific variations of the phenomena observed.

ACKNOWLEDGMENTS

We thank Walter Holzer and Jutta Hutecek for their excellent technical assistance.

This work was supported by the Austrian Science Fund FWF (projects P17035-B09 and P25265-B21).

REFERENCES

1. **Plotkin SA, Orenstein WA, Offit PA.** 2013. Vaccines, 6th ed. Saunders Elsevier, San Diego, CA.
2. **Grun JL, Maurer PH.** 1989. Different T helper cell subsets elicited in mice utilizing two different adjuvant vehicles: the role of endogenous interleukin 1 in proliferative responses. Cell Immunol. **121:**134–145.
3. **Mannhalter JW, Neychev HO, Zlabinger GJ, Ahmad R, Eibl MM.** 1985. Modulation of the human immune response by the non-toxic and non-pyrogenic adjuvant aluminium hydroxide: effect on antigen uptake and antigen presentation. Clin. Exp. Immunol. **61:**143–151.
4. **Morefield GL, Sokolovska A, Jiang D, HogenEsch H, Robinson JP, Hem**

SL. 2005. Role of aluminum-containing adjuvants in antigen internalization by dendritic cells in vitro. Vaccine **23:**1588–1595.
5. **Eisenbarth SC, Colegio OR, O'Connor W, Sutterwala FS, Flavell RA.** 2008. Crucial role for the Nalp3 inflammasome in the immunostimulatory properties of aluminium adjuvants. Nature **453:**1122–1126.
6. **Li H, Willingham SB, Ting JP, Re F.** 2008. Cutting edge: inflammasome activation by alum and alum's adjuvant effect are mediated by NLRP3. J. Immunol. **181:**17–21.
7. **Kool M, Petrilli V, De Smedt T, Rolaz A, Hammad H, van Nimwegen M, Bergen IM, Castillo R, Lambrecht BN, Tschopp J.** 2008. Cutting edge: alum adjuvant stimulates inflammatory dendritic cells through activation of the NALP3 inflammasome. J. Immunol. **181:**3755–3759.
8. **McKee AS, Munks MW, MacLeod MK, Fleenor CJ, Van Rooijen N, Kappler JW, Marrack P.** 2009. Alum induces innate immune responses through macrophage and mast cell sensors, but these sensors are not required for alum to act as an adjuvant for specific immunity. J. Immunol. **183:**4403–4414.
9. **Franchi L, Nunez G.** 2008. The Nlrp3 inflammasome is critical for aluminium hydroxide-mediated IL-1beta secretion but dispensable for adjuvant activity. Eur. J. Immunol. **38:**2085–2089.
10. **Flach TL, Ng G, Hari A, Desrosiers MD, Zhang P, Ward SM, Seamone ME, Vilaysane A, Mucsi AD, Fong Y, Prenner E, Ling CC, Tschopp J, Muruve DA, Amrein MW, Shi Y.** 2011. Alum interaction with dendritic cell membrane lipids is essential for its adjuvanticity. Nat. Med. **17:**479–487.
11. **De Gregorio E, Tritto E, Rappuoli R.** 2008. Alum adjuvanticity: unraveling a century old mystery. Eur. J. Immunol. **38:**2068–2071.
12. **Marichal T, Ohata K, Bedoret D, Mesnil C, Sabatel C, Kobiyama K, Lekeux P, Coban C, Akira S, Ishii KJ, Bureau F, Desmet CJ.** 2011. DNA released from dying host cells mediates aluminum adjuvant activity. Nat. Med. **17:**996–1002.
13. **McKee AS, Burchill MA, Munks MW, Jin L, Kappler JW, Friedman RS, Jacobelli J, Marrack P.** 2013. Host DNA released in response to aluminum adjuvant enhances MHC class II-mediated antigen presentation and prolongs CD4 T-cell interactions with dendritic cells. Proc. Natl. Acad. Sci. U. S. A. **110:**E1122–E1131.
14. **Gupta RK.** 1998. Aluminum compounds as vaccine adjuvants. Adv. Drug Deliv. Rev. **32:**155–172.
15. **Jones LS, Peek LJ, Power J, Markham A, Yazzie B, Middaugh CR.** 2005. Effects of adsorption to aluminum salt adjuvants on the structure and stability of model protein antigens. J. Biol. Chem. **280:**13406–13414.
16. **Wagner L, Verma A, Meade BD, Reiter K, Narum DL, Brady RA, Little SF, Burns DL.** 2012. Structural and immunological analysis of anthrax recombinant protective antigen adsorbed to aluminum hydroxide adjuvant. Clin. Vaccine Immunol. **19:**1465–1473.
17. **Iyer V, Hu L, Liyanage MR, Esfandiary R, Reinisch C, Meinke A, Maisonneuve J, Volkin DB, Joshi SB, Middaugh CR.** 2012. Preformulation characterization of an aluminum salt-adjuvanted trivalent recombinant protein-based vaccine candidate against Streptococcus pneumoniae. J. Pharm. Sci. **101:**3078–3090.
18. **Ljutic B, Ochs M, Messham B, Ming M, Dookie A, Harper K, Ausar SF.** 2012. Formulation, stability and immunogenicity of a trivalent pneumococcal protein vaccine formulated with aluminum salt adjuvants. Vaccine **30:**2981–2988.
19. **Fauquet CM, Mayo MA, Maniloff J, Desselberger U, Ball LA.** 2005. Virus taxonomy. Elsevier Inc, San Diego, CA.
20. **Lindenbach BD, Thiel H-J, Rice CM.** 2007. Flaviviridae: the viruses and their replication, p 1101–1152. *In* Knipe DM, Howley PM (ed), Fields virology, 5th ed. Lippincott Williams & Wilkins Co, Philadelphia, PA.
21. **Nybakken GE, Nelson CA, Chen BR, Diamond MS, Fremont DH.** 2006. Crystal structure of the West Nile virus envelope glycoprotein. J. Virol. **80:**11467–11474.
22. **Rey FA, Heinz FX, Mandl C, Kunz C, Harrison SC.** 1995. The envelope glycoprotein from tick-borne encephalitis virus at 2 A resolution. Nature **375:**291–298.
23. **Kanai R, Kar K, Anthony K, Gould LH, Ledizet M, Fikrig E, Marasco WA, Koski RA, Modis Y.** 2006. Crystal structure of West Nile virus envelope glycoprotein reveals viral surface epitopes. J. Virol. **80:**11000–11008.
24. **Luca VC, AbiMansour J, Nelson CA, Fremont DH.** 2012. Crystal structure of the Japanese encephalitis virus envelope protein. J. Virol. **86:**2337–2346.
25. **Modis Y, Ogata S, Clements D, Harrison SC.** 2003. A ligand-binding pocket in the dengue virus envelope glycoprotein. Proc. Natl. Acad. Sci. U. S. A. **100:**6986–6991.
26. **Kuhn RJ, Zhang W, Rossmann MG, Pletnev SV, Corver J, Lenches E, Jones CT, Mukhopadhyay S, Chipman PR, Strauss EG, Baker TS, Strauss JH.** 2002. Structure of dengue virus: implications for flavivirus organization, maturation, and fusion. Cell **108:**717–725.
27. **Mukhopadhyay S, Kim BS, Chipman PR, Rossmann MG, Kuhn RJ.** 2003. Structure of West Nile virus. Science **302:**248.
28. **Zhang X, Ge P, Yu X, Brannan JM, Bi G, Zhang Q, Schein S, Zhou ZH.** 2013. Cryo-EM structure of the mature dengue virus at 3.5-A resolution. Nat. Struct. Mol. Biol. **20:**105–110.
29. **Zhang X, Sheng J, Plevka P, Kuhn RJ, Diamond MS, Rossmann MG.** 2013. Dengue structure differs at the temperatures of its human and mosquito hosts. Proc. Natl. Acad. Sci. U. S. A. **110:**6795–6799.
30. **Fibriansah G, Ng TS, Kostyuchenko VA, Lee J, Lee S, Wang J, Lok SM.** 2013. Structural changes of dengue virus when exposed to a temperature of 37°C. J. Virol. **87:**7585–7592.
31. **Barrett AD, Teuwen DE.** 2009. Yellow fever vaccine–how does it work and why do rare cases of serious adverse events take place? Curr. Opin. Immunol. **21:**308–313.
32. **Kreil TR, Burger I, Bachmann M, Fraiss S, Eibl MM.** 1997. Antibodies protect mice against challenge with tick-borne encephalitis virus (TBEV)-infected macrophages. Clin. Exp. Immunol. **110:**358–361.
33. **Pierson TC, Diamond MS.** 2008. Molecular mechanisms of antibody-mediated neutralisation of flavivirus infection. Expert Rev. Mol. Med. **10:**e12. doi:10.1017/S1462399408000665.
34. **Pierson TC, Fremont DH, Kuhn RJ, Diamond MS.** 2008. Structural insights into the mechanisms of antibody-mediated neutralization of flavivirus infection: implications for vaccine development. Cell Host Microbe **4:**229–238.
35. **Zlatkovic J, Stiasny K, Heinz FX.** 2011. Immunodominance and functional activities of antibody responses to inactivated West Nile virus and recombinant subunit vaccines in mice. J. Virol. **85:**1994–2003.
36. **Oliphant T, Nybakken GE, Austin SK, Xu Q, Bramson J, Loeb M, Throsby M, Fremont DH, Pierson TC, Diamond MS.** 2007. Induction of epitope-specific neutralizing antibodies against West Nile virus. J. Virol. **81:**11828–11839.
37. **Wahala WM, Kraus AA, Haymore LB, Accavitti-Loper MA, de Silva AM.** 2009. Dengue virus neutralization by human immune sera: role of envelope protein domain III-reactive antibody. Virology **392:**103–113.
38. **Lai CY, Tsai WY, Lin SR, Kao CL, Hu HP, King CC, Wu HC, Chang GJ, Wang WK.** 2008. Antibodies to envelope glycoprotein of dengue virus during the natural course of infection are predominantly cross-reactive and recognize epitopes containing highly conserved residues at the fusion loop of domain II. J. Virol. **82:**6631–6643.
39. **Beltramello M, Williams KL, Simmons CP, Macagno A, Simonelli L, Quyen NT, Sukupolvi-Petty S, Navarro-Sanchez E, Young PR, de Silva AM, Rey FA, Varani L, Whitehead SS, Diamond MS, Harris E, Lanzavecchia A, Sallusto F.** 2010. The human immune response to Dengue virus is dominated by highly cross-reactive antibodies endowed with neutralizing and enhancing activity. Cell Host Microbe **8:**271–283.
40. **Vratskikh O, Stiasny K, Zlatkovic J, Tsouchnikas G, Jarmer J, Karrer U, Roggendorf M, Roggendorf H, Allwinn R, Heinz FX.** 2013. Dissection of antibody specificities induced by yellow Fever vaccination. PLoS Pathog. **9:**e1003458. doi:10.1371/journal.ppat.1003458.
41. **Sanchez MD, Pierson TC, Degrace MM, Mattei LM, Hanna SL, Del Piero F, Doms RW.** 2007. The neutralizing antibody response against West Nile virus in naturally infected horses. Virology **359:**336–348.
42. **Oliphant T, Engle M, Nybakken GE, Doane C, Johnson S, Huang L, Gorlatov S, Mehlhop E, Marri A, Chung KM, Ebel GD, Kramer LD, Fremont DH, Diamond MS.** 2005. Development of a humanized monoclonal antibody with therapeutic potential against West Nile virus. Nat. Med. **11:**522–530.
43. **Heinz FX, Kunz C.** 1981. Homogeneity of the structural glycoprotein from European isolates of tick-borne encephalitis virus: comparison with other flaviviruses. J. Gen. Virol. **57:**263–274.
44. **Maizel JV.** 1971. Polyacrylamide gel electrophoresis of viral proteins. Methods Virol. **5:**179–246.
45. **Heinz FX, Stiasny K, Puschner-Auer G, Holzmann H, Allison SL, Mandl CW, Kunz C.** 1994. Structural changes and functional control of the tick-borne encephalitis virus glycoprotein E by the heterodimeric association with protein prM. Virology **198:**109–117.
46. **Kiermayr S, Stiasny K, Heinz FX.** 2009. Impact of quaternary organiza-

tion on the antigenic structure of the tick-borne encephalitis virus envelope glycoprotein E. J. Virol. **83:**8482–8491.
47. **Stiasny K, Kiermayr S, Holzmann H, Heinz FX.** 2006. Cryptic properties of a cluster of dominant flavivirus cross-reactive antigenic sites. J. Virol. **80:**9557–9568.
48. **Frey A, Di Canzio J, Zurakowski D.** 1998. A statistically defined endpoint titer determination method for immunoassays. J. Immunol. Methods **221:** 35–41.
49. **Puschnik A, Lau L, Cromwell EA, Balmaseda A, Zompi S, Harris E.** 2013. Correlation between dengue-specific neutralizing antibodies and serum avidity in primary and secondary dengue virus 3 natural infections in humans. PLoS Negl. Trop. Dis. **7:**e2274. doi:10.1371/journal.pntd.0002274.
50. **Guisasola ME, Ramos B, Sanz JC, Garcia-Bermejo I, De Ory Manchon F.** 2010. Comparison of IgG avidity assays in the confirmation of the diagnosis of cytomegalovirus primary infection. APMIS **118:**991–993.
51. **Robertson P, Beynon S, Whybin R, Brennan C, Vollmer-Conna U, Hickie I, Lloyd A.** 2003. Measurement of EBV-IgG anti-VCA avidity aids the early and reliable diagnosis of primary EBV infection. J. Med. Virol. **70:**617–623.
52. **Stiasny K, Holzmann H, Heinz FX.** 2009. Characteristics of antibody responses in tick-borne encephalitis vaccination breakthroughs. Vaccine **27:**7021–7026.
53. **Heinz FX, Tuma W, Guirakhoo F, Kunz C.** 1986. A model study of the use of monoclonal antibodies in capture enzyme immunoassays for antigen quantification exploiting the epitope map of tick-borne encephalitis virus. J. Biol. Stand. **14:**133–141.
54. **Kenney JS, Hughes BW, Masada MP, Allison AC.** 1989. Influence of adjuvants on the quantity, affinity, isotype and epitope specificity of murine antibodies. J. Immunol. Methods **121:**157–166.
55. **Schallert N, Pihlgren M, Kovarik J, Roduit C, Tougne C, Bozzotti P, Del Giudice G, Siegrist CA, Lambert PH.** 2002. Generation of adult-like antibody avidity profiles after early-life immunization with protein vaccines. Eur. J. Immunol. **32:**752–760.
56. **Olafsdottir TA, Lingnau K, Nagy E, Jonsdottir I.** 2012. Novel protein-based pneumococcal vaccines administered with the Th1-promoting adjuvant IC31 induce protective immunity against pneumococcal disease in neonatal mice. Infect. Immun. **80:**461–468.
57. **Gromowski GD, Barrett ND, Barrett AD.** 2008. Characterization of dengue virus complex-specific neutralizing epitopes on envelope protein domain III of dengue 2 virus. J. Virol. **82:**8828–8837.
58. **Nybakken GE, Oliphant T, Johnson S, Burke S, Diamond MS, Fremont DH.** 2005. Structural basis of West Nile virus neutralization by a therapeutic antibody. Nature **437:**764–769.
59. **Mandl CW, Guirakhoo F, Holzmann H, Heinz FX, Kunz C.** 1989. Antigenic structure of the flavivirus envelope protein E at the molecular level, using tick-borne encephalitis virus as a model. J. Virol. **63:**564–571.
60. **Guirakhoo F, Heinz FX, Kunz C.** 1989. Epitope model of tick-borne encephalitis virus envelope glycoprotein E: analysis of structural properties, role of carbohydrate side chain, and conformational changes occurring at acidic pH. Virology **169:**90–99.
61. **Lindblad EB.** 2004. Aluminium compounds for use in vaccines. Immunol. Cell Biol. **82:**497–505.
62. **Hogenesch H.** 2012. Mechanism of immunopotentiation and safety of aluminum adjuvants. Front. Immunol. **3:**406.
63. **Sukupolvi-Petty S, Austin SK, Purtha WE, Oliphant T, Nybakken GE, Schlesinger JJ, Roehrig JT, Gromowski GD, Barrett AD, Fremont DH, Diamond MS.** 2007. Type- and subcomplex-specific neutralizing antibodies against domain III of dengue virus type 2 envelope protein recognize adjacent epitopes. J. Virol. **81:**12816–12826.
64. **Beasley DW, Barrett AD.** 2002. Identification of neutralizing epitopes within structural domain III of the West Nile virus envelope protein. J. Virol. **76:**13097–13100.
65. **Wuorimaa T, Dagan R, Vakevainen M, Bailleux F, Haikala R, Yaich M, Eskola J, Kayhty H.** 2001. Avidity and subclasses of IgG after immunization of infants with an 11-valent pneumococcal conjugate vaccine with or without aluminum adjuvant. J. Infect. Dis. **184:**1211–1215.
66. **Lofgren JA, Dhandapani S, Pennucci JJ, Abbott CM, Mytych DT, Kaliyaperumal A, Swanson SJ, Mullenix MC.** 2007. Comparing ELISA and surface plasmon resonance for assessing clinical immunogenicity of panitumumab. J. Immunol. **178:**7467–7472.
67. **Lok SM, Kostyuchenko V, Nybakken GE, Holdaway HA, Battisti AJ, Sukupolvi-Petty S, Sedlak D, Fremont DH, Chipman PR, Roehrig JT, Diamond MS, Kuhn RJ, Rossmann MG.** 2008. Binding of a neutralizing antibody to dengue virus alters the arrangement of surface glycoproteins. Nat. Struct. Mol. Biol. **15:**312–317.
68. **Chang M, Shi Y, Nail SL, HogenEsch H, Adams SB, White JL, Hem SL.** 2001. Degree of antigen adsorption in the vaccine or interstitial fluid and its effect on the antibody response in rabbits. Vaccine **19:**2884–2889.
69. **Iyer S, HogenEsch H, Hem SL.** 2003. Relationship between the degree of antigen adsorption to aluminum hydroxide adjuvant in interstitial fluid and antibody production. Vaccine **21:**1219–1223.
70. **Morefield GL, Jiang D, Romero-Mendez IZ, Geahlen RL, Hogenesch H, Hem SL.** 2005. Effect of phosphorylation of ovalbumin on adsorption by aluminum-containing adjuvants and elution upon exposure to interstitial fluid. Vaccine **23:**1502–1506.
71. **Flarend RE, Hem SL, White JL, Elmore D, Suckow MA, Rudy AC, Dandashli EA.** 1997. In vivo absorption of aluminium-containing vaccine adjuvants using 26Al. Vaccine **15:**1314–1318.
72. **Holzmann H, Mandl CW, Guirakhoo F, Heinz FX, Kunz C.** 1989. Characterization of antigenic variants of tick-borne encephalitis virus selected with neutralizing monoclonal antibodies. J. Gen. Virol. **70**(Part 1)**:**219–222.